

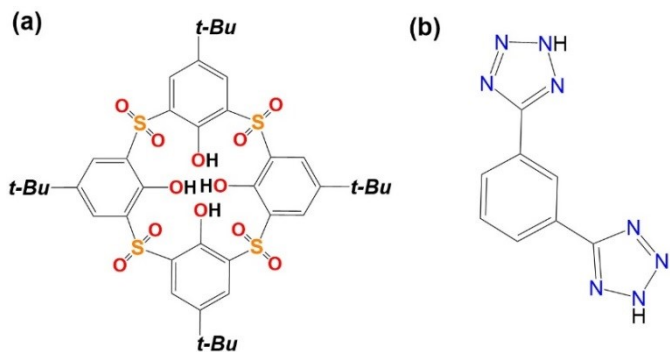
Thiacalixarene-based $\{\text{Co}/\text{Fe}\}_{16}$ molecular clusters: the bimetallic synergistic effect for enhanced oxygen evolution reduction

Xinxin Hang^{a,b}, Xiaoju Wang^a, Meiling, Wang,^b Mengwei Chen^b, Yanfeng Bi^{*b}

^a School of Chemistry and Chemical Engineering, Institute for Innovative Materials and Energy, Yangzhou University, Yangzhou, Jiangsu 225002, (P. R. China)

^b School of Petrochemical Engineering, Liaoning Petrochemical University, Fushun, Liaoning 113001 (P. R. China)

Additional Figures



Scheme S1. Molecular structures of $\text{H}_4\text{TC4A-SO}_2$ (a) and H_2BTTAB (b).

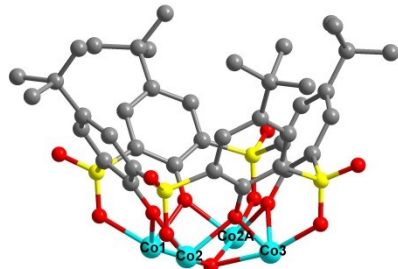


Figure S1. The structure of $\text{Co}_4\text{-(TC4A-SO}_2)$ PSBU.

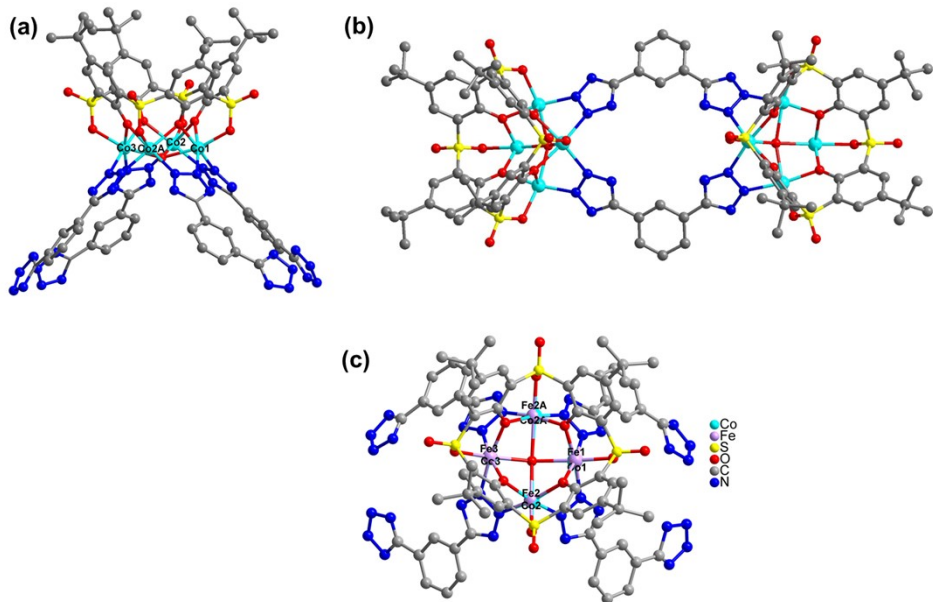


Figure S2. The coordination modes of (a) $\text{Co}_4\text{-(TC4A-SO}_2)$ unit, (b) BTTAB ligand in Co_{16} and (c) $(\text{Co/Fe})_4\text{-(TC4A-SO}_2)$ unit in $\{\text{CoFe}\}_{16}\text{-b}$. Symmetry operators for equivalent positions are as follows: $A = x, 1-y, 1-z$ for Co_{16} and $A = x, y, 2-z$ for $\{\text{CoFe}\}_{16}\text{-b}$. Based on the single-crystal X-ray diffraction analysis, the ratio of Co and Fe is 3:2 in $\{\text{CoFe}\}_{16}\text{-b}$.

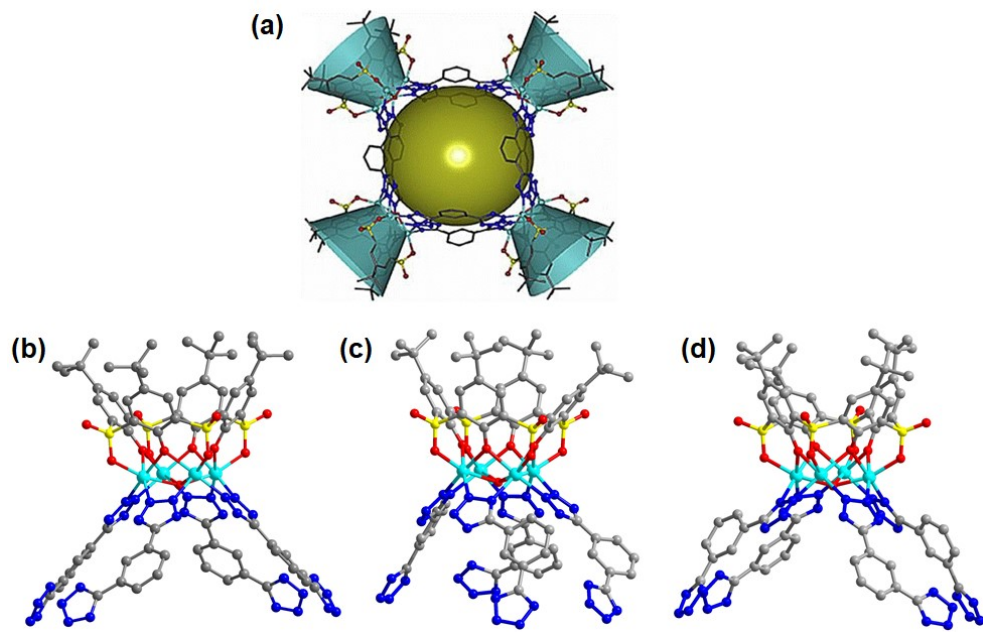


Figure S3. (a) $\{Co_{16}\}$ architecture (in literature) assembled from Co₄-(TC4A-SO₂) SBUs and BTTAB. (b-d) The coordination modes of Co₄-(TC4A-SO₂) units.

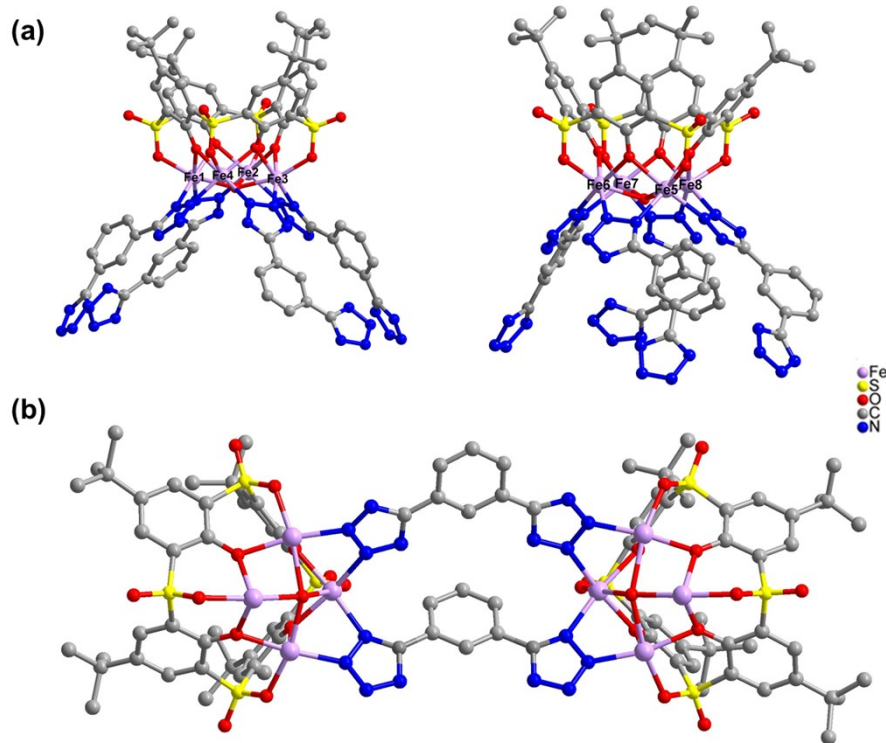


Figure S4. The coordination modes of two Fe₄-(TC4A-SO₂) units (a) and BTTAB ligand (b) in Fe₁₆.

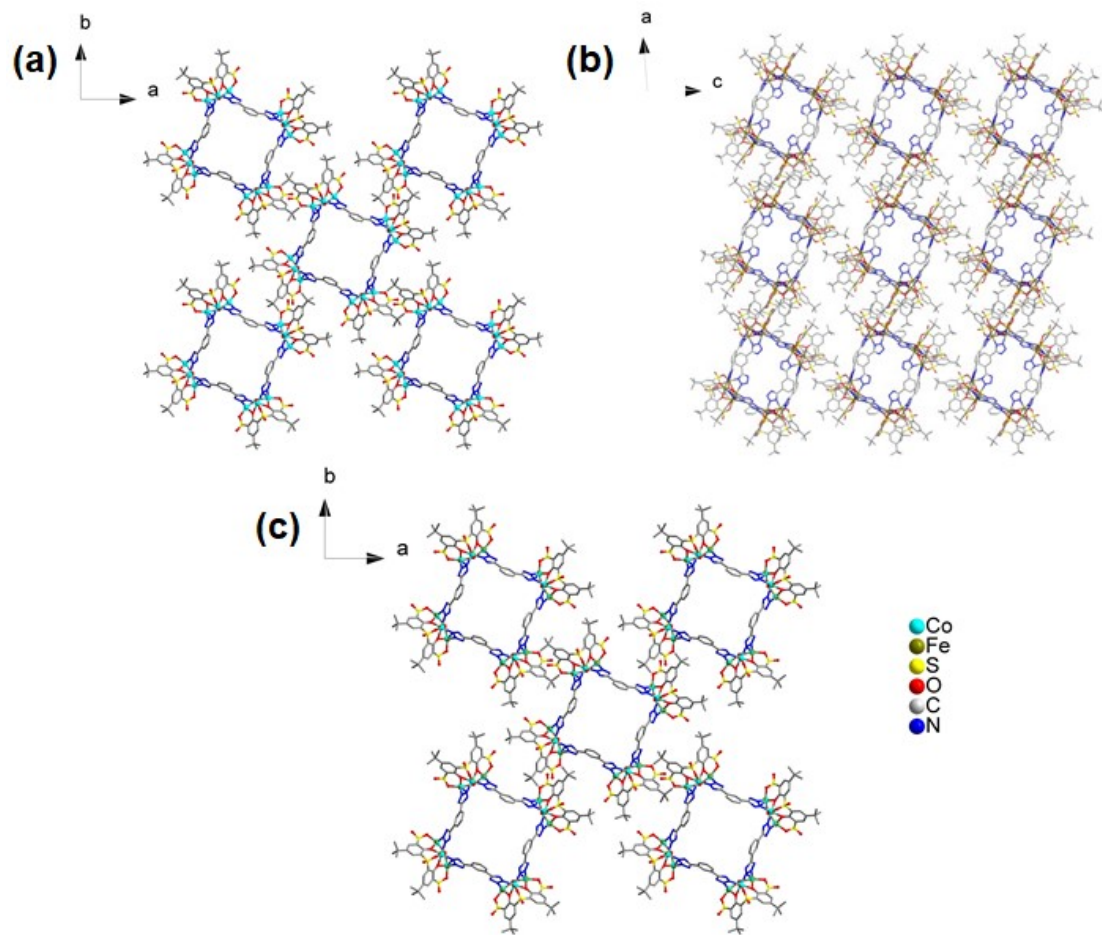


Figure S5. The packing diagrams of Co_{16} (a), Fe_{16} (b) and $\{\text{CoFe}\}_{16-\mathbf{b}}$ (c).

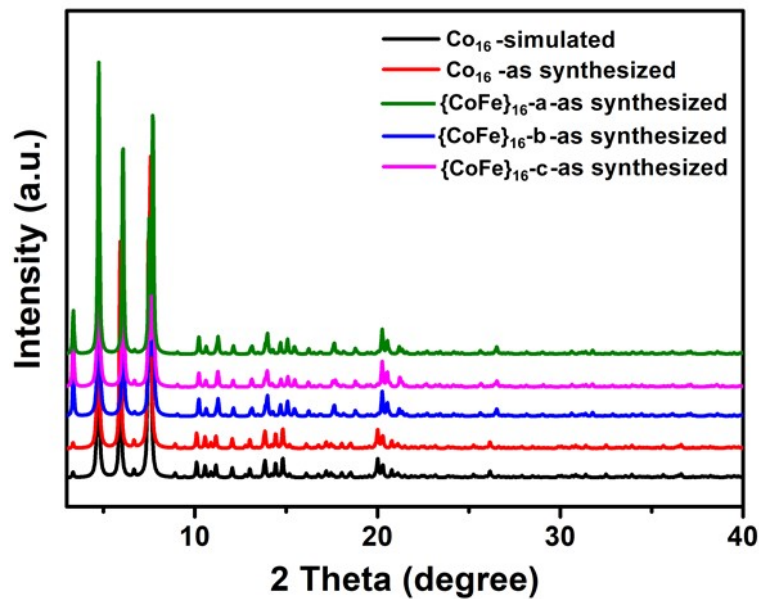


Figure S6. PXRD patterns of Co_{16} , $\{\text{CoFe}\}_{16}\text{-a}$, $\{\text{CoFe}\}_{16}\text{-b}$, and $\{\text{CoFe}\}_{16}\text{-c}$.

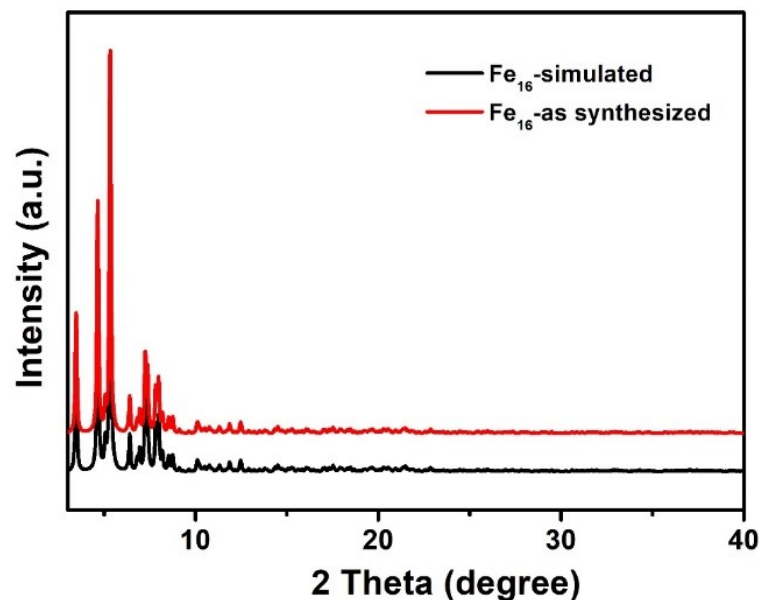


Figure S7. PXRD pattern of Fe_{16} .

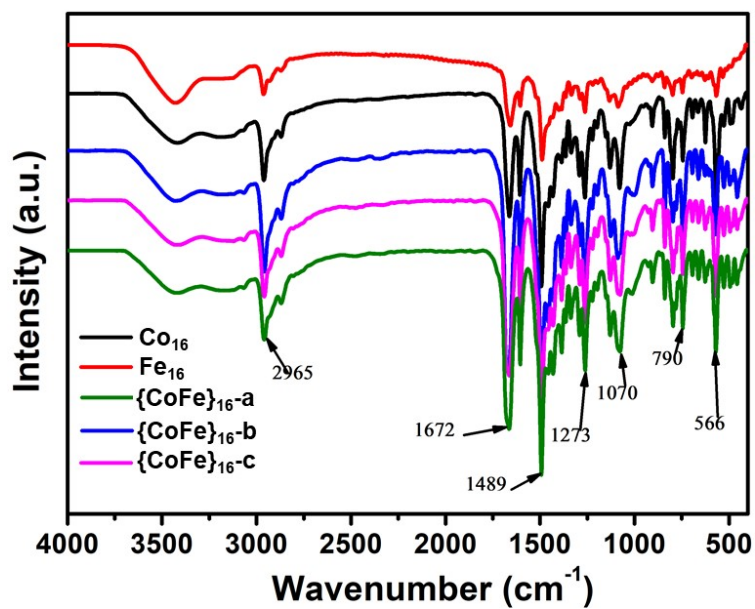


Figure S8. FT-IR spectra of Co_{16} , Fe_{16} , $\{\text{CoFe}\}_{16\text{-a}}$, $\{\text{CoFe}\}_{16\text{-b}}$, and $\{\text{CoFe}\}_{16\text{-c}}$.

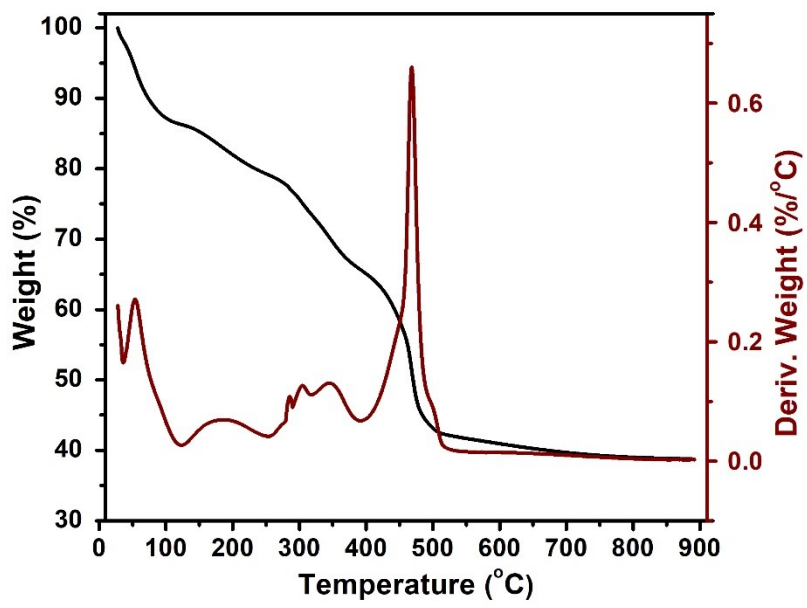


Figure S9. TGA curves of Co_{16} .

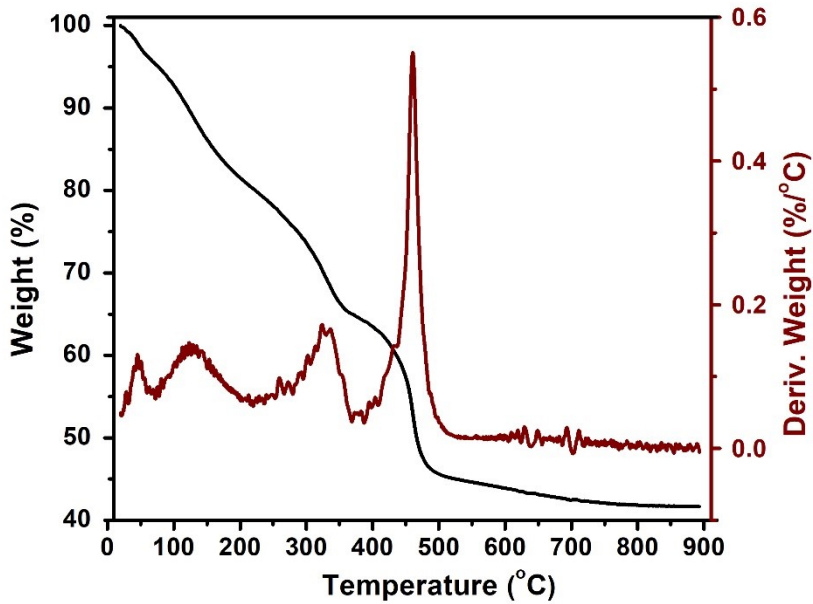


Figure S10. TGA curves of $\{\text{CoFe}\}_{16\text{-b}}$.

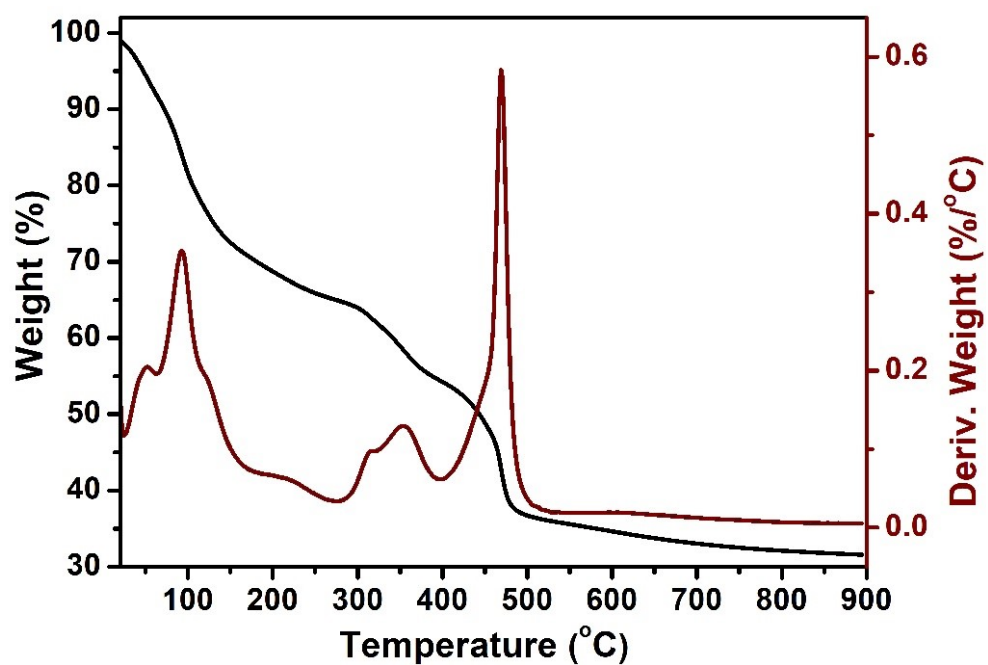


Figure S11. TGA curves of Fe_{16} .

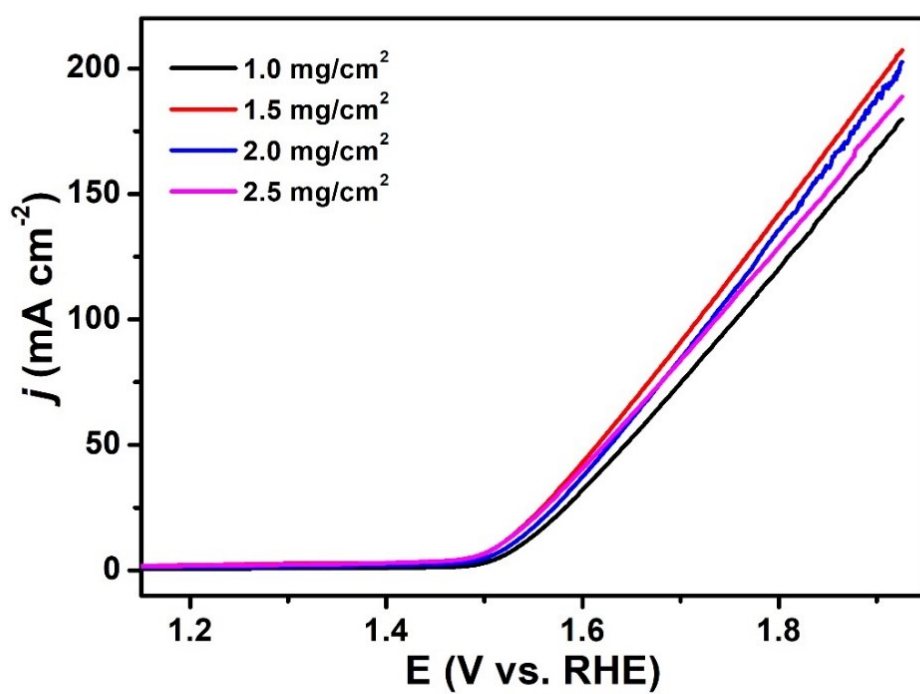


Figure S12. LSV curves of $\{\text{CoFe}\}_{16\text{-b}}/\text{CP}$ at different loading.

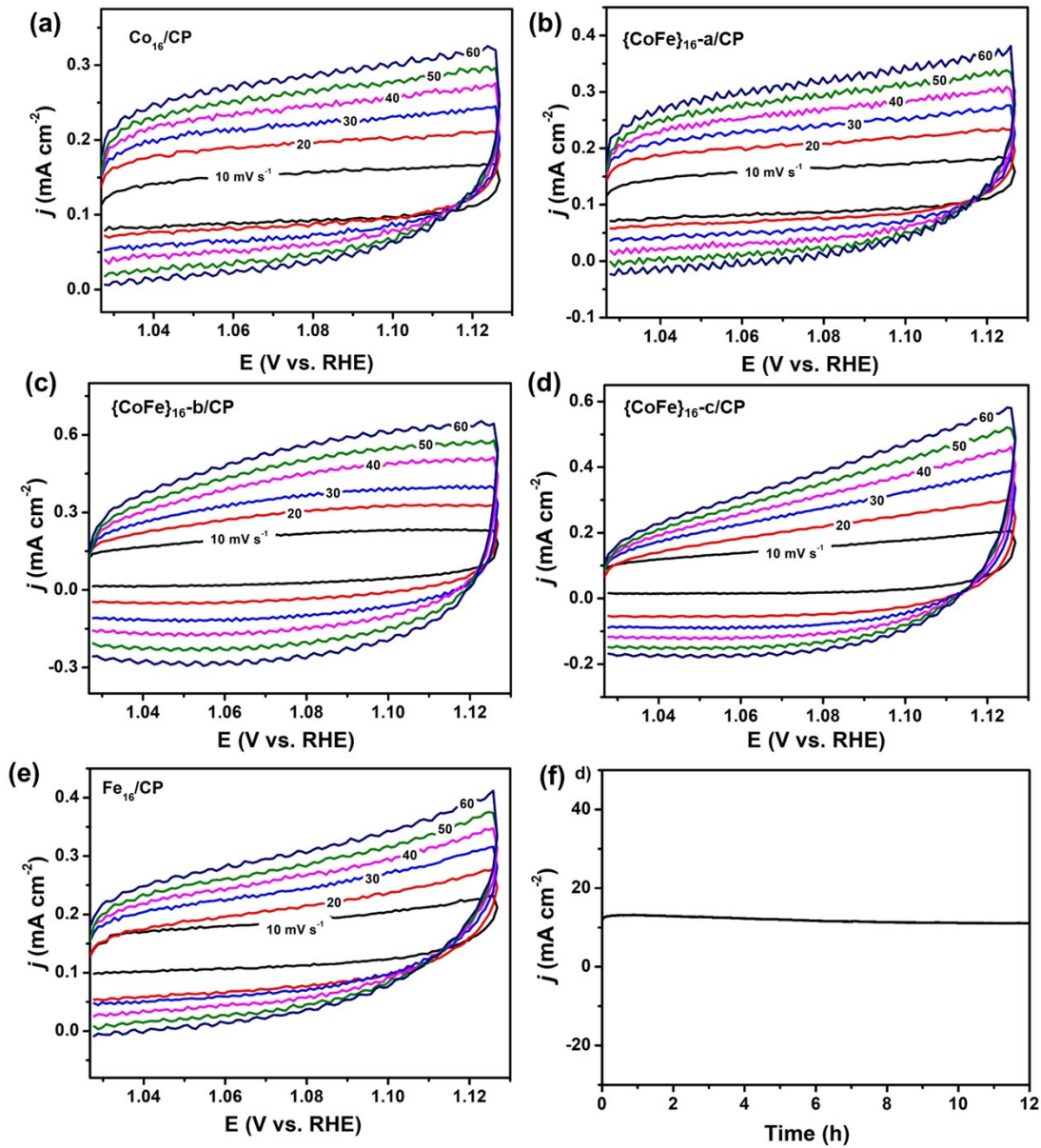


Figure S13. Cyclic voltammetry (CV) curves of Co_{16}/CP (a), $\{\text{CoFe}\}_{16-\text{a}}/\text{CP}$ (b), $\{\text{CoFe}\}_{16-\text{b}}/\text{CP}$ (c), $\{\text{CoFe}\}_{16-\text{c}}/\text{CP}$ (d) and Fe_{16}/CP (e); (f) i - t curve of the $\{\text{CoFe}\}_{16-\text{b}}/\text{CP}$ catalyst recorded at 1.60 V vs RHE.

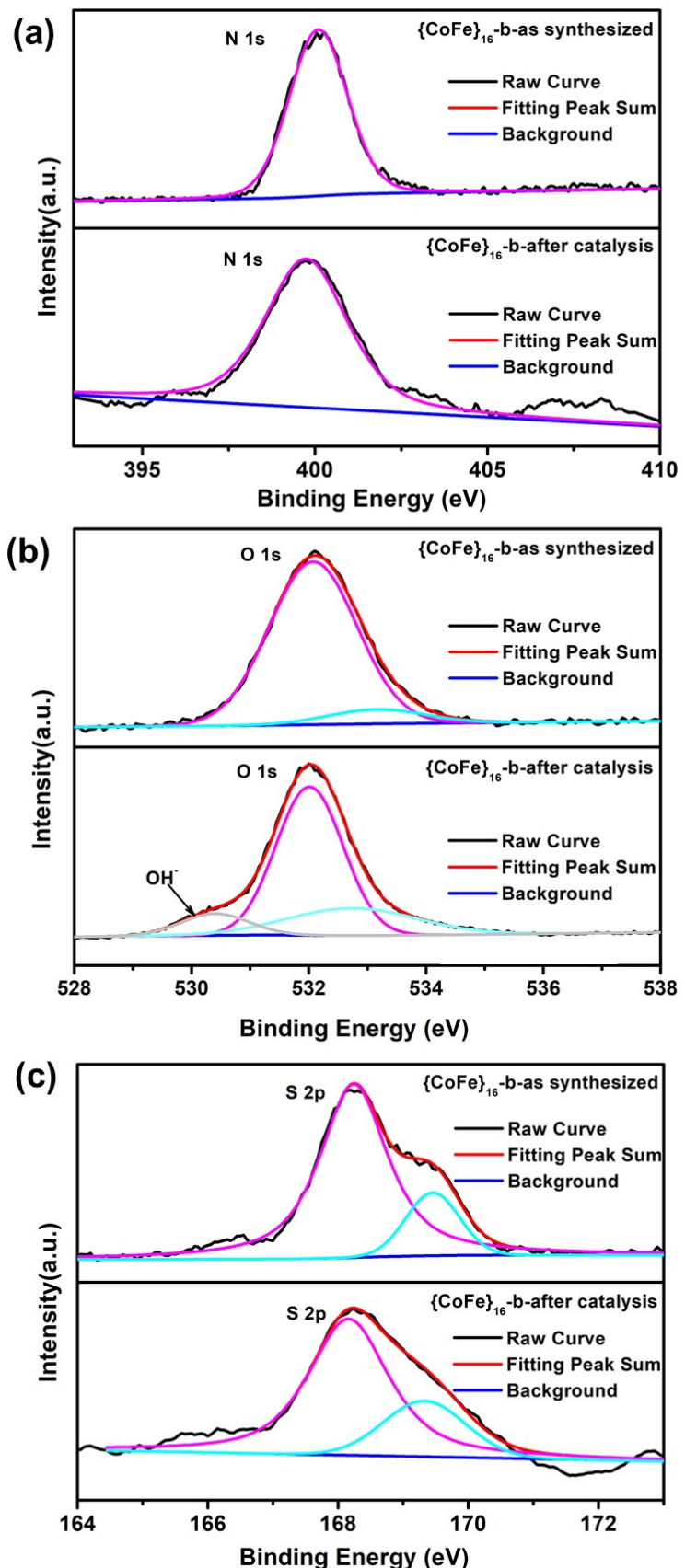


Figure S14. High-resolution N 1s (a), O 1s (b), and S 2p (c) XPS spectra of as-synthesized {CoFe}₁₆-b and {CoFe}₁₆-b after catalysis (after stabilized LSV).

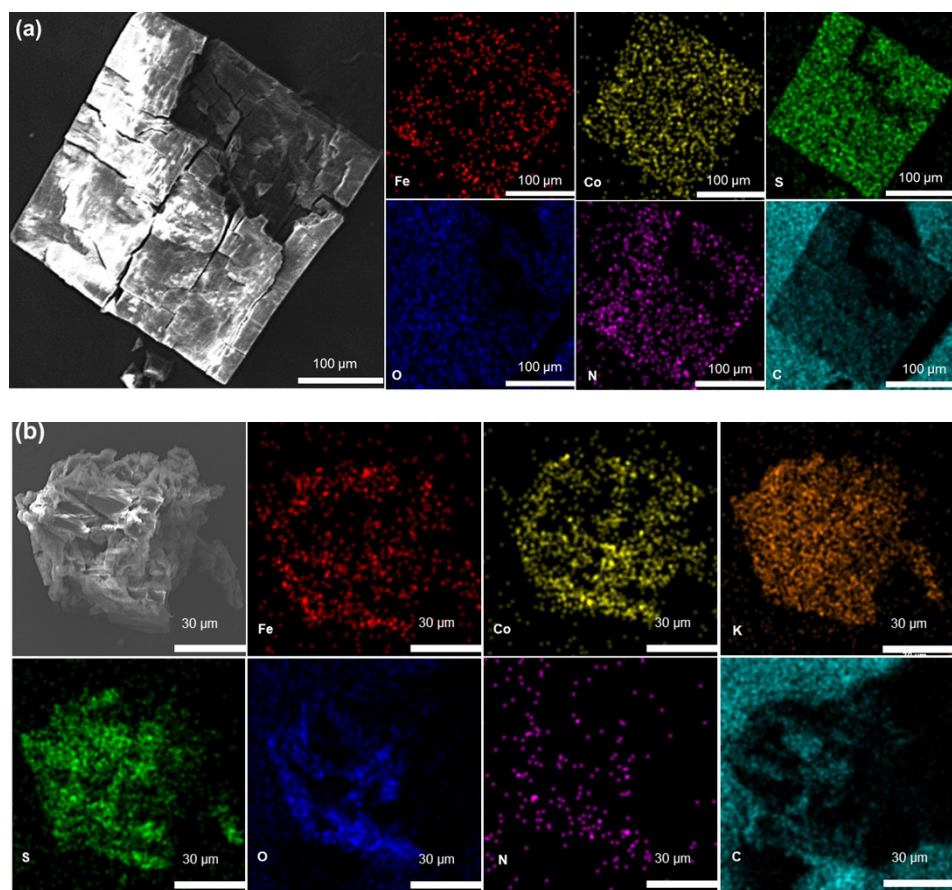


Figure S15. Scanning electron microscope (SEM) elemental mapping images of $\{CoFe\}_{16}\text{-b}$ at different stage: (a) $\{CoFe\}_{16}\text{-b}$ -as-prepared, (b) $\{CoFe\}_{16}\text{-b}$ after OER catalysis.

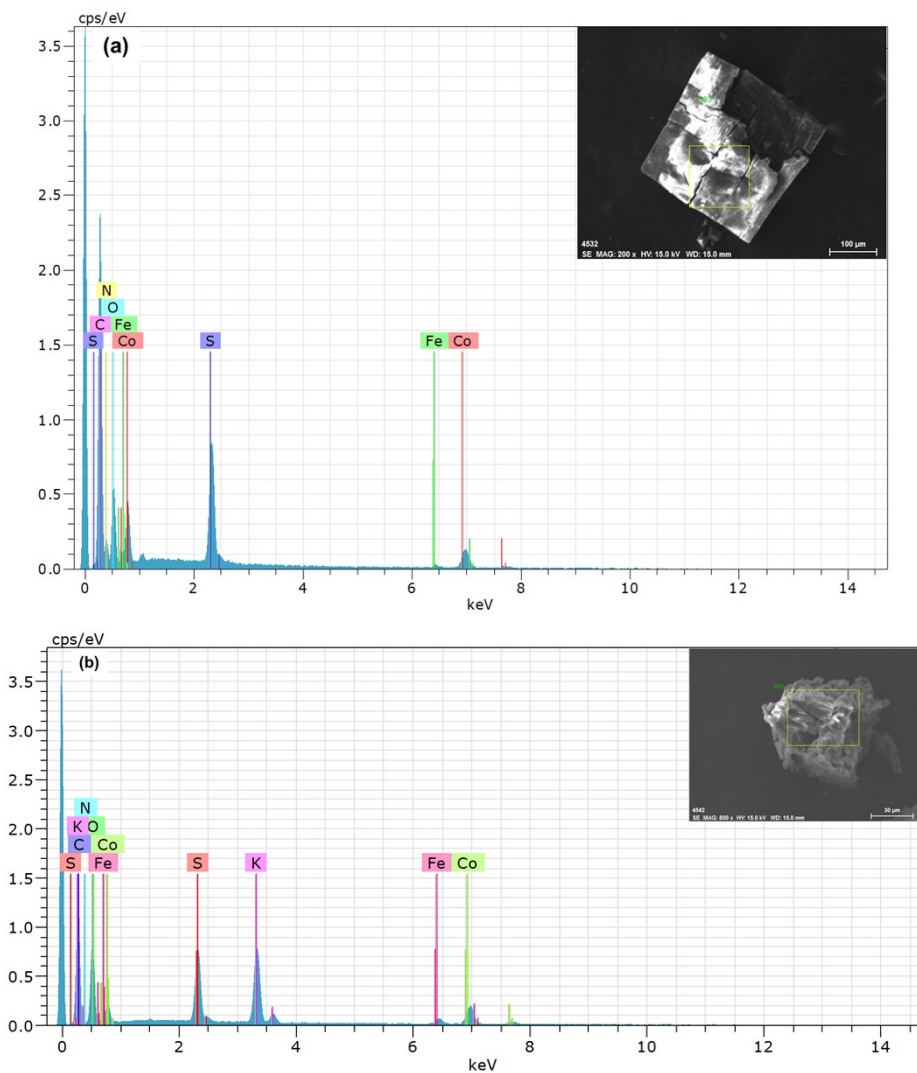


Figure S16. Energy-dispersive X-ray spectroscopy (EDS) analysis of $\{CoFe\}_{16}\text{-b}$ at different stage: (a) $\{CoFe\}_{16}\text{-b}$ -as-prepared, (b) $\{CoFe\}_{16}\text{-b}$ after OER catalysis.

Table S1. Selected Crystal Data for Clusters **Co₁₆**, **Fe₁₆** and **{CoFe}₁₆-b**.

	Co₁₆	Fe₁₆	{CoFe}₁₆-b
Formula*	C ₂₂₄ H ₂₁₆ N ₆₄ Co ₁₆ O ₅₂ S ₁₆	C ₂₂₄ H ₂₁₆ N ₆₄ Fe ₁₆ O ₅₂ S ₁₆	C ₂₂₄ H ₂₁₆ N ₆₄ Co _{9.60} Fe _{6.40} O ₅₂ S ₁₆
Formula Weight*	6092.44	6035.27	6072.72
Crystal System	Tetragonal	Monoclinic	Tetragonal
Space Group (no.)	<i>I</i> 4/ <i>m</i> (No. 87)	<i>C</i> 2/ <i>c</i> (No. 15)	<i>I</i> 4/ <i>m</i> (No. 87)
Temperature (K)	150 K	150 K	150 K
<i>a</i> (Å)	37.4109(13)	51.070(3)	37.212(3)
<i>b</i> (Å)	37.4109(13)	17.5178(11)	37.212(3)
<i>c</i> (Å)	16.2505(7)	52.146(3)	15.8033(13)
α (°)	90	90	90
β (°)	90	94.784(2)	90
γ (°)	90	90	90
<i>V</i> (Å ³)	22743.8(19)	46489(5)	21883(4)
<i>Z</i>	2	4	2
<i>D_c</i> (g/cm ⁻³) *	0.890	0.862	0.920
μ (mm ⁻¹)	0.689	0.602	0.685
<i>F</i> (000)	6224	12352	6195
Total Data	36053	132196	51005
Unique data	7443	34333	10093
<i>R</i> _{int}	0.070	0.0752	0.067
<i>GOF</i> on <i>F</i> ²	1.03	1.00	1.026
<i>R</i> ₁ ^a [<i>I</i> >2 σ(<i>I</i>)]	0.0559	0.0599	0.0611
<i>wR</i> ₂ ^b	0.1933	0.1798	0.2115

^a*R*₁=Σ||*F*₀|-|*F*_c||/Σ|*F*₀|; ^b*wR*₂={Σ[*w(F*₀²-*F*_c²)²]}/{Σ[*w(F*₀²)²]})^{1/2}

Table S2. Selected bond distances (\AA) and BVS calculations for **Co₁₆**, **{CoFe}₁₆-b**, and **Fe₁₆**

Fe ₁₆							
Band	Distance	r	Value	Band	Distance	r	Value
Fe(1)-O(5)	2.060(3)	1.73	0.414	Fe(5)-O(17)	2.097(3)	1.73	0.394
Fe(1)-N(10)	2.119(4)	1.86	0.497	Fe(5)-O(13)	2.118(3)	1.73	0.354
Fe(1)-O(4)	2.131(3)	1.73	0.342	Fe(5)-N(14)	2.125(4)	1.86	0.489
Fe(1)-O(25)	2.138(3)	1.73	0.336	Fe(5)-O(26)	2.166(3)	1.73	0.311
Fe(1)-N(1)	2.161(4)	1.86	0.443	Fe(5)-N(5)	2.182(4)	1.86	0.419
Fe(1)-O(1)	2.197(3)	1.73	0.286	Fe(5)-O(16)	2.211(3)	1.73	0.275
valence			2.318	valence			2.242
Fe(2)-O(2)	2.057(3)	1.73	0.418	Fe(6)-O(19)	2.095(3)	1.73	0.377
Fe(2)-N(11)	2.100(4)	1.86	0.523	Fe(6)-O(13)	2.103(3)	1.73	0.369
Fe(2)-O(7)	2.109(3)	1.73	0.363	Fe(6)-N(6)	2.110(4)	1.86	0.509
Fe(2)-N(30) ^a	2.123(4)	1.86	0.491	Fe(6)-O(14)	2.119(3)	1.73	0.353
Fe(2)-O(1)	2.146(3)	1.73	0.328	Fe(6)-N(26)	2.123(4)	1.86	0.491
Fe(2)-O(25)	2.264(3)	1.73	0.239	Fe(6)-O(26)	2.190(3)	1.73	0.292
valence			2.362	valence			2.391
Fe(3)-O(9)	2.062(3)	1.73	0.412	Fe(7)-O(21)	2.088(3)	1.73	0.384
Fe(3)-O(25)	2.135(3)	1.73	0.338	Fe(7)-O(15)	2.106(3)	1.73	0.366
Fe(3)-O(2)	2.145(3)	1.73	0.329	Fe(7)-N(23) ^a	2.118(4)	1.86	0.498
Fe(3)-N(19)	2.147(4)	1.86	0.460	Fe(7)-N(25)	2.030(5)	1.86	0.481
Fe(3)-N(29) ^a	2.166(4)	1.86	0.437	Fe(7)-O(14)	2.139(3)	1.73	0.335
Fe(3)-O(3)	2.198(3)	1.73	0.285	Fe(7)-O(26)	2.2532(3)	1.73	0.246
valence			2.263	valence			2.309
Fe(4)-O(4)	2.047(3)	1.73	0.429	Fe(8)-O(23)	2.076(3)	1.73	0.397
Fe(4)-N(18)	2.088(4)	1.86	0.540	Fe(8)-O(15)	2.091(3)	1.73	0.381
Fe(4)-O(11)	2.107(3)	1.73	0.365	Fe(8)-N(22) ^a	2.105(4)	1.86	0.516
Fe(4)-O(3)	2.110(3)	1.73	0.362	Fe(8)-N(15)	2.110(4)	1.86	0.509
Fe(4)-N(2)	2.127(4)	1.86	0.486	Fe(8)-O(16)	2.110(3)	1.73	0.362
Fe(4)-O(25)	2.308(3)	1.73	0.212	Fe(8)-O(26)	2.616(2)	1.73	0.262
valence			2.394	valence			2.426
Symmetry Code a: 3/2-x,3/2-y,1-z.							

Note: BVS calculations reveal that all the ions in these clusters are divalent.

Table S3. ICP-AES analysis of catalysts {CoFe}₁₆-a, {CoFe}₁₆-b, and {CoFe}₁₆-c.

Catalysts	Co (ppm)	Fe (ppm)	Co: Fe (molar ratio)	Experimental value
{CoFe} ₁₆ -a	1362.0	56.55	24.10 : 1	Co _{15.4} Fe _{0.6}
{CoFe} ₁₆ -b	977.6	635.1	1.54 : 1	Co _{9.7} Fe _{6.3}
{CoFe} ₁₆ -c	639.5	910.9	1 : 1.42	Co _{6.4} Fe _{9.6}